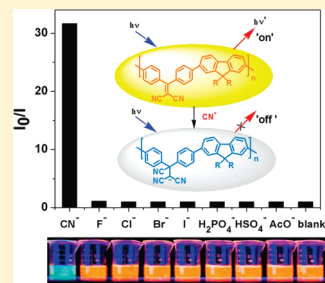


Highly Selective and Sensitive Detection of Cyanide by a Reaction-Based Conjugated Polymer Chemosensor

Xiaofu Wu,^{†,‡} Bowei Xu,^{†,‡} Hui Tong,^{*,†} and Lixiang Wang^{*,†}[†]State Key Laboratory of Polymer Physics and Chemistry, Changchun Institute of Applied Chemistry, Chinese Academy of Sciences, Changchun 130022, P. R. China[‡]Graduate School, Chinese Academy of Sciences, Beijing 100039, P. R. China

Supporting Information

ABSTRACT: Based on a specific nucleophilic addition reaction with cyanide, a dicyano-vinyl-containing conjugated polymer (**P1**) has been designed and synthesized as a colorimetric and fluorescent chemosensor for cyanide anion. The combination of advantages of both reaction-based sensors and conjugated polymer sensors offers its highly sensitive and selective recognition of CN^- . The addition of CN^- to **P1** solution induced a change in the solution color from yellow-green to colorless, while no color change could be observed in presence of other common anions, by which CN^- can be identified from other anions directly with the naked eye. At the same time, a 31.6-fold fluorescence quenching was achieved upon adding CN^- into **P1** solution. The fluorescence quenching has shown a linear response to CN^- in the concentration range of 0.5–30 μM . Furthermore, its detection limit for CN^- can be as low as 14 ppb, which is among the best results for the fluorescent conjugated polymer-based cyanide chemosensors. Compared with its small molecular counterpart, **P1** exhibits higher sensitivity and selectivity, wider linear region, and faster response.



INTRODUCTION

Conjugated polymer (CP) fluorescent chemosensors have attracted much attention in these years due to their higher sensitivity over model compounds based on the molecular wire effect.¹ Compared with lots of good CP fluorescence sensors for cationic or neutral species, the development of anion CP sensors is still far behind, although many anions are important in numerous biological and chemical processes. As most of small molecule anion sensors,² CP-based anion sensors have been achieved by covalent or noncovalent (displacement approach) binding of anion receptors to conjugated polymers.^{3–5} While most CP-based anion sensors are highly sensitive, their selectivity is often insufficient. For example, fluoride, cyanide, and acetate anions always lead to similar spectral changes for hydrogen bonding based anion sensors,⁴ and the sensing behaviors of metal complex based anion sensors can be disturbed by other coordination ligands and even metal ions.⁵

Cyanide is an extremely toxic anion and can directly lead to the death of human beings in several minutes. Nevertheless, cyanide salts are still widely used as industrial materials in gold mining, electroplating, plastics production, and other fields.⁶ Therefore, the World Health Organization (WHO) has set the maximum contaminant level (MCL) of 2.7 μM (70 ppb) for cyanide in drinking water.⁷ Among various colorimetric and fluorescent sensors for cyanide, chemodosimetric sensors relied on cyanide's exceptional nucleophilicity always show very high selectivity.^{6,8} However, the rather low sensitivity and reactivity of these sensors are still serious problems. Thus, it is reasonable to develop CP-based chemodosimetric sensors for cyanide detection, which will

exhibit both the high sensitivity of CP-based sensors and the high selectivity of chemodosimetric sensors. To our surprise, this desirable combination of these sensing properties has not been mentioned at all for the reaction-based conjugated polymer fluoride sensor reported by Swager et al.⁹

In this contribution, we designed and synthesized a novel conjugated polyfluorene (**P1**) containing dicyano-vinyl unit in its main chain as a highly selective and sensitive cyanide sensor. Its design is based on the consideration that the dicyano-vinyl group can act as a selective cyanide-reactive unit for the nucleophilic addition reaction,¹⁰ which may break the effective conjugation of polymer main chain and influence the electronic structure and optical properties of **P1** (Scheme 1). Meanwhile, because of the exciton-transporting properties of CPs, the charged nucleophilic adducts can act as trapping sites in the polymer main chains, which may amplify the fluorescence quenching effect. Thus, it is reasonably predicted that **P1** will exhibit higher sensitivity toward CN^- compared to its model compound **M1**.

EXPERIMENTAL SECTION

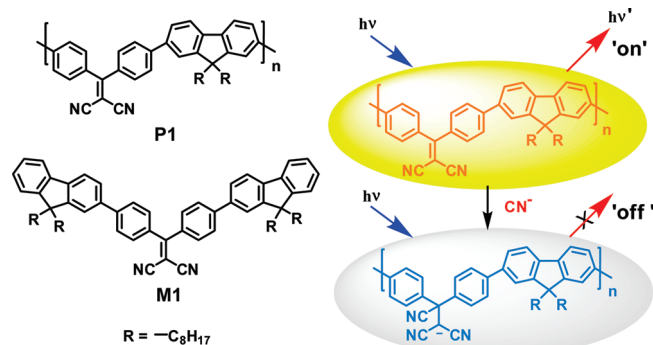
Materials. All chemicals and reagents were used as received from commercial sources without further purification. Solvents for chemical synthesis were purified according to standard procedures. Monomer 9,9-dioctylfluorene-2,7-bis(trimethylene boronate)¹¹ and

Received: March 13, 2011

Revised: April 28, 2011

Published: May 11, 2011

Scheme 1. Structures of P1 and M1 and the Sensing Mechanism of P1



9,9-dioctylfluorene-2-trimethylene boronate¹² were synthesized as previously described.

Measurement and Characterization. ¹H and ¹³C NMR spectra were recorded on a Bruker AV-300 with CDCl₃ or DMSO-*d*₆ as solvents. IR spectra were obtained on a FT-IR Bruker Vertex 70 spectrometer at a nominal resolution of 2 cm⁻¹. The power samples were prepared by adding model compounds and polymers into KBr, and the mixture was ground to a fine powder and pressed to form a disk. Molecular mass spectra of model compound and its precursor were recorded on a LDI-1700 MALDI-TOF mass spectrometer. Molecular weight and polydispersity of the polymers were determined by gel permeation chromatography (GPC) on a Waters 410 instrument with polystyrene as standards and THF as eluent. UV-vis absorption measurements were carried out on Perkin-Elmer Lambda 35 UV-vis spectrometer, with a scan rate of 500 nm/min. Fluorescence emission spectra were recorded on a Perkin-Elmer LS 50B fluorescence spectrometer with xenon discharge lamp excitation.

Fluorescence Titration Procedure. A 10 × 10 mm quartz cuvette was used for solution spectra, and emission was collected at 90° relative to the excitation beam. The solutions of polymer **P1** and model compound **M1** were successive diluted to a concentration of 5 × 10⁻⁶ M in *N,N*-dimethylformamide (DMF) (the concentration of polymers is based on the moles of the repeated unit). The photoluminescent quantum yields were determined in DMF at 293 K against 10⁻⁵ M quinine sulfate in 1.0 N H₂SO₄ solution as a reference standard (Φ_F = 0.546). Solutions of anionic tetrabutylammonium salts with the concentration of typically 1 × 10⁻² M were prepared in DMF. Fluorescence intensity changes of **P1** and **M1** were recorded before and after additions of 30 μL of the anionic solutions into 3.00 mL of the **P1** and **M1** solutions. The tetrabutylammonium cyanide stock solution of 1 × 10⁻² M was diluted to 1.0 × 10⁻³, 1.0 × 10⁻⁴, and 1.0 × 10⁻⁵ M with DMF, respectively. Fluorescent responses to the varied concentrations of cyanide ion were conducted by adding small aliquots of cyanide solutions to 3.00 mL of the **P1** and **M1** solutions.

Synthesis. **Polymer P0.** A mixture of 4,4'-dibromobenzophenone (0.17 g, 0.5 mmol), 9,9-dioctylfluorene-2,7-bis(trimethylene boronate) (0.279 g, 0.5 mmol), and Pd(PPh₃)₄ (2.3 mg) was added and degassed for 30 min. Then a solution of 2.0 M aqueous K₂CO₃ (2 mL) and toluene (6 mL) was injected via syringe, and the reaction mixture was degassed and stirred at 90 °C for 20 h under an argon atmosphere. After cooling to room temperature, the resulting mixture was diluted in dichloromethane. The solution was washed with brine and deionized water. The separated organic layer was dried with anhydrous Na₂SO₄. After filtration, the solvent was removed, and the residue was redissolved with a minimum amount of dichloromethane and precipitated in methanol. The resulting off-white polymers were obtained after drying in vacuum with a yield of 88% (0.25 g). ¹H NMR (CDCl₃, 300 MHz): δ (ppm): 7.99 (d, 4H, *J* = 8.2), 7.87–7.82 (m, 6H), 7.71–7.67 (m, 4H),

2.09 (br, 4H), 1.09 (m, 20H), 0.80–0.66 (m, 10H). ¹³C NMR (CDCl₃, 100 MHz): δ (ppm): 195.8, 152.0, 145.6, 140.7, 139.0, 136.3, 130.7, 127.0, 126.4, 121.7, 120.4, 121.6, 120.4, 55.5, 40.3, 31.7, 30.0, 29.2, 23.8, 22.6, 14.0. FT-IR (cm⁻¹): 3032, 2926, 2853, 1657, 1602, 1555, 1465, 1402, 1282, 1181, 1109, 1016, 930, 819, 770. GPC (THF, polystyrene standard), *M*_n: 59.0 kDa; *M*_w: 113.8 kDa; PDI: 1.93.

Polymer P1. The polymer **P0** (0.15 g, 0.26 mmol) and malononitrile (0.170 g, 2.6 mmol) were dissolved in 25 mL of dry dichloromethane. After the mixture was cooled to 0 °C under an argon atmosphere, titanium tetrachloride (0.28 mL, 2.6 mmol) was added dropwise and stirred at this temperature for 30 min. While the solution was maintained at 0 °C, pyridine (0.56 mL, 6.9 mmol) was added dropwise and stirred at this temperature for 30 min. Then, the cooling bath was removed, and the solution was heated to reflux for 24 h. After cooling to room temperature, the reaction mixture was poured into dichloromethane and then washed with 10% HCl solution and 10% NaHCO₃ solution. The solution was dried with Na₂SO₄. After filtration, the solvent was removed, and the residue was redissolved with a minimum amount of dichloromethane and precipitated in methanol. The resulting yellow polymers were obtained after drying in vacuum with a yield of 87% (0.14 g). ¹H NMR (CDCl₃, 300 MHz): 7.79–7.74 (m, 6H), 7.61–7.55 (m, 8H), 2.06 (br, 4H), 1.02 (m, 20H), 0.74–0.64 (m, 10H). ¹³C NMR (CDCl₃, 100 MHz): δ (ppm): 174.0, 152.2, 146.0, 141.8, 138.7, 134.7, 131.3, 126.4, 121.7, 120.0, 114.4, 55.5, 40.4, 31.7, 30.0, 29.2, 23.8, 22.6, 14.0. FT-IR (cm⁻¹): 3032, 2926, 2853, 2224, 1600, 1561, 1466, 1405, 1328, 1260, 1181, 1095, 1015, 814, 753. GPC (THF, polystyrene standard), *M*_n: 59.3 kDa; *M*_w: 109.1 kDa; PDI: 1.84.

4,4'-Bis(9,9-di-*n*-octylfluorene-2-yl)benzophenone (M0). A mixture of 4,4'-dibromobenzophenone (0.34 g, 1 mmol), 9,9-dioctylfluorene-2-trimethylene boronate (1.04 g, 2.2 mmol), and Pd(PPh₃)₄ (20 mg) was added and degassed for 30 min. Then a solution of 2.0 M aqueous K₂CO₃ (16 mL) and toluene (16 mL) was injected via syringe, and the reaction mixture was degassed and stirred at 90 °C for 20 h under an argon atmosphere. After cooling to room temperature, the resulting mixture was diluted in dichloromethane. The solution was washed with brine and deionized water. The separated organic layer was dried with anhydrous Na₂SO₄. After filtration, the solvent was removed and the crude product was purified by column chromatography using petroleum ether/dichloromethane = 2:1 (v/v) as eluent, and the white power was obtained after drying in vacuum with a yield of 80% (0.77 g). ¹H NMR (CDCl₃, 400 MHz) δ (ppm): 7.97 (d, 4H, *J* = 7.9 Hz), 7.81–7.79 (m, 6H), 7.75 (m, 2H), 7.65 (dd, 2H, *J* = 7.9 Hz, *J* = 1.4 Hz), 7.62 (s, 2H), 7.38–7.31 (m, 6H), 2.02 (m, 8H), 1.06 (m, 40H), 0.80 (t, 12H), 0.68 (br, 8H). ¹³C NMR (CDCl₃, 100 MHz): 195.8, 151.6, 151.1, 145.7, 141.4, 140.5, 138.7, 136.2, 130.7, 127.4, 127.0, 126.9, 126.2, 122.9, 121.6, 120.1, 55.2, 40.3, 31.7, 30, 29.2, 23.8, 22.6, 14.0. FT-IR (cm⁻¹): 3036, 2925, 2852, 1638, 1601, 1555, 1466, 1401, 1285, 1185, 1013, 932, 864, 739. *m/z* [MALDI-TOF]: 959.7 [M + H]⁺.

1,1-Bis(4,4'-bis(9,9-di-*n*-octylfluorene-2-yl)phenyl)-2,2-dicyanoethylene (M1). The compound **M0** (0.4 mg, 0.41 mmol) and malononitrile (0.132 g, 2.0 mmol) were dissolved in 30 mL of dry dichloromethane. After the mixture was cooled to 0 °C under an argon atmosphere, titanium tetrachloride (0.26 mL, 2.4 mmol) was added dropwise and stirred at this temperature for 30 min. While the solution was maintained at 0 °C, pyridine (0.52 mL, 6.5 mmol) was added dropwise and stirred at this temperature for 30 min. Then, the cooling bath was removed, and the solution was heated to reflux overnight. After cooling to room temperature, the reaction mixture was poured into dichloromethane and filtered through a pad of silica gel. The solution was washed with 10% HCl solution and 10% NaHCO₃ solution. The solution was dried with Na₂SO₄. After filtration, the solvent was removed and the crude product was purified by column chromatography using petroleum ether/dichloromethane = 2:1 (v/v) as eluent, and the yellow solid was obtained after dry in vacuum with a yield of 60% (0.25 g). ¹H NMR (CDCl₃,

400 MHz): δ (ppm): 7.81–7.78 (m, 6H), 7.80 (m, 6H), 7.63–7.60 (m, 8H), 7.38–7.31 (m, 6H), 2.01 (m, 8H), 1.05 (m, 40H), 0.80 (t, 12H), 0.66 (br, 8H). ^{13}C NMR (CDCl_3 , 100 MHz): 174.0, 151.7, 151.1, 146.2, 141.8, 140.3, 139.0, 134.6, 131.3, 127.5, 127.3, 126.9, 126.1, 122.9, 121.5, 120.0, 114.4, 55.2, 40.3, 31.7, 30, 29.2, 23.8, 22.6, 14.0. FT-IR (cm^{-1}): 3036, 2926, 2853, 2223, 1601, 1560, 1531, 1452, 1404, 1329, 1285, 1181, 1014, 822, 740. m/z [MALDI-TOF]: 1007.7 $[\text{M} + \text{H}]^+$.

RESULTS AND DISCUSSION

Synthesis and Structure Characterization. The synthetic procedure for polymer **P1** is shown in Scheme 2. Initially, the precursor polymer **P0** was obtained from the Suzuki coupling polycondensation between dibromobenzophenone and 9,9-dioctylfluorene-2,7-bis(trimethylene boronate) with a yield of 88%. Subsequently, **P0** was further condensed with malononitrile by using a titanium-mediated Knoevenagel condensation reaction to afford the final polymer **P1** in 87% yield. For comparison, model compound **M1** was prepared by Suzuki cross-coupling reactions of dibromobenzophenone with 9,9-dioctylfluorene-2-trimethylene boronate, followed by a Knoevenagel condensation reaction with malononitrile.

The structures of polymer **P1** and model compound **M1** were verified by ^1H NMR, ^{13}C NMR, FT-IR, and MALDI-TOF mass spectrometry (for **M1**). The complete conversion of the precursor polymer **P0** containing carbonyl group into **P1** containing dicyano-vinyl group was revealed by FT-IR and ^{13}C NMR. The IR characteristic absorption peaks of aromatic carbonyl group for **P0** appeared at 1694 cm^{-1} . After condensation reaction, this characteristic absorption of carbonyl disappeared completely. Concomitantly, new absorption peak at 2217 cm^{-1} for **P1** emerged, which was assigned to $\text{C}\equiv\text{N}$ stretching vibration of the nitrile group. Furthermore, the complete disappearances of the carbonyl carbon atom signal at 195.8 ppm and the appearances of olefinic carbon atom signals at 174.0 ppm and nitrile carbon atom signals at 114.4 ppm in the ^{13}C NMR confirmed the efficient condensation reaction. The polymer **P1** and **P0** could

dissolve in common organic solvents such as chloroform and THF. They were also soluble in polar solvent DMF but insoluble in methanol. By gel permeation chromatography (GPC) using polystyrene standards, the number-average molecular weights of **P1** and **P0** were determined to be 59.0 kDa with polydispersity index (PDI) value of 1.93 and 59.3 kDa with PDI value of 1.84, respectively.

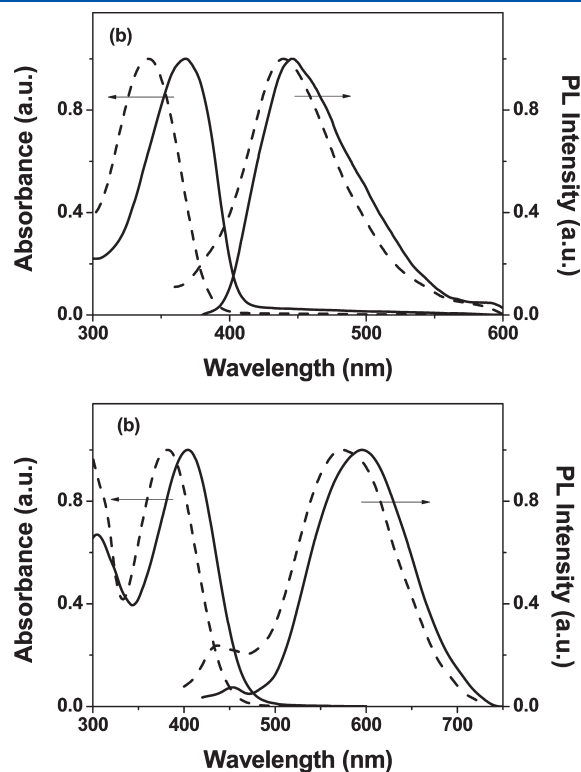
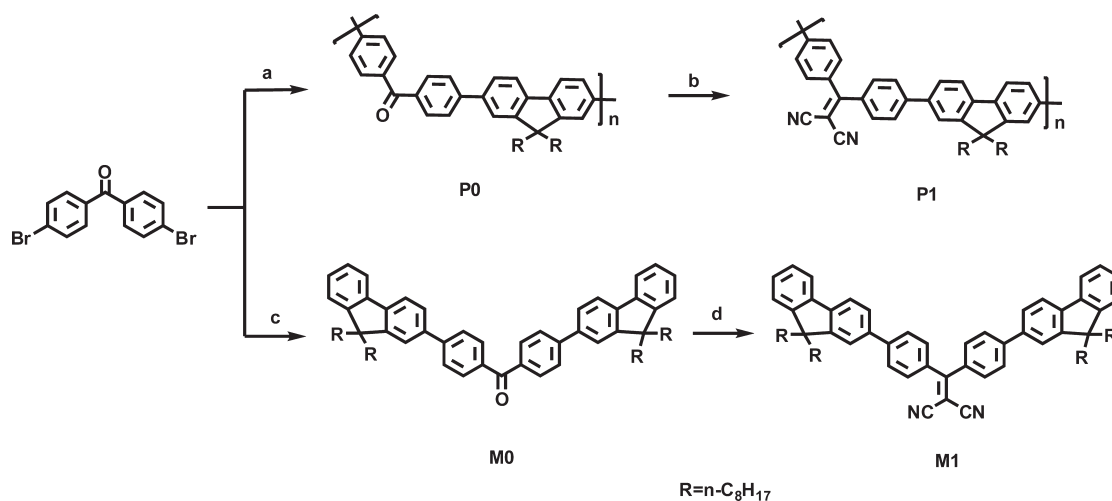


Figure 1. (a) UV–vis absorption and PL spectra of **M0** (dash line) and **P0** (solid line) in DMF. (b) UV–vis absorption and PL spectra of **M1** (dash line) and **P1** (solid line) in DMF.

Scheme 2. Synthesis Procedures of **P1** and **M1**^a



^a Reagent and conditions: (a) 9,9-dioctylfluorene-2,7-bis(trimethylene boronate), $\text{Pd}(\text{PPh}_3)_4$, K_2CO_3 (2 M), toluene, 90°C , 48 h, 88%; (b) malononitrile, TiCl_4 , pyridine, $0-60^\circ\text{C}$, 24 h, 87%; (c) 9,9-dioctylfluorene-2-trimethylene boronate, $\text{Pd}(\text{PPh}_3)_4$, K_2CO_3 (2 M), toluene, 90°C , 20 h, 80%; (d) malononitrile, TiCl_4 , pyridine, $0-60^\circ\text{C}$, overnight, 60%.

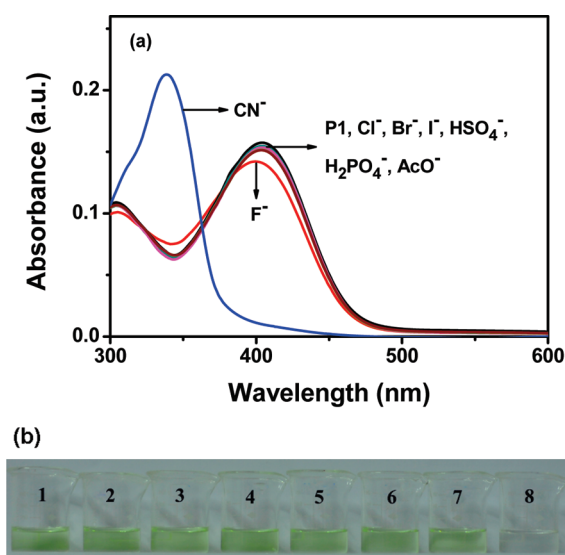


Figure 2. (a) UV-vis absorption changes of **P1** ($5\ \mu\text{M}$) upon addition of 20 equiv of each anion as Bu_4N^+ salts in DMF within 10 min. (b) Visible images observed for **P1** solutions upon addition of each anion: 1, F^- ; 2, Cl^- ; 3, Br^- ; 4, I^- ; 5, HSO_4^- ; 6, H_2PO_4^- ; 7, AcO^- ; 8, CN^- ; 9, **P1** only.

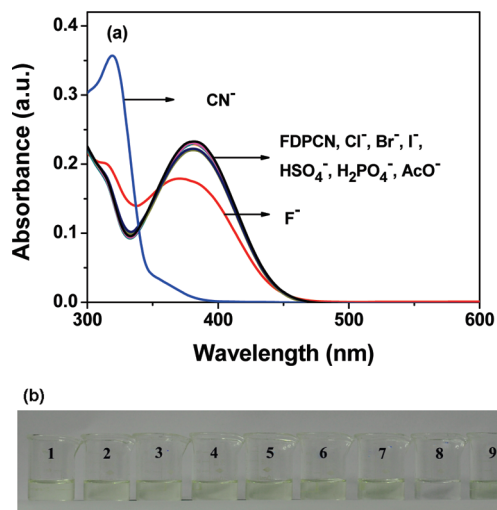


Figure 3. (a) UV-vis absorption changes of **M1** ($5\ \mu\text{M}$) upon addition of 20 equiv of each anion in DMF within 10 min. (b) Visible images observed for **M1** solutions upon addition of each anion: 1, F^- ; 2, Cl^- ; 3, Br^- ; 4, I^- ; 5, HSO_4^- ; 6, H_2PO_4^- ; 7, AcO^- ; 8, CN^- ; 9, **M1** only.

Photophysical Properties. The absorption and emission spectra of **P1** and **M1** and their precursors (**P0** and **M0**) were measured in DMF at a concentration of $5\ \mu\text{M}$ (Table S1 in Supporting Information). Both **M0** and **P0** solutions were colorless and showed blue emission. As shown in Figure 1a, the absorption and emission maxima of **M0** solution were at 340 and 438 nm, respectively, while those of **P0** were red-shifted to 368 and 446 nm, respectively, due to the increased conjugation of polymer backbone. Relative to the absorption peaks of **M0** and **P0**, the absorption spectra of **M1** and **P1** only red-shifted for 12 and 20 nm with the peaks at 380 and 403 nm, respectively. Their solutions were light yellow for **M1** and yellow-green for **P1**. On the other hand, the emission spectra of model compound **M1**

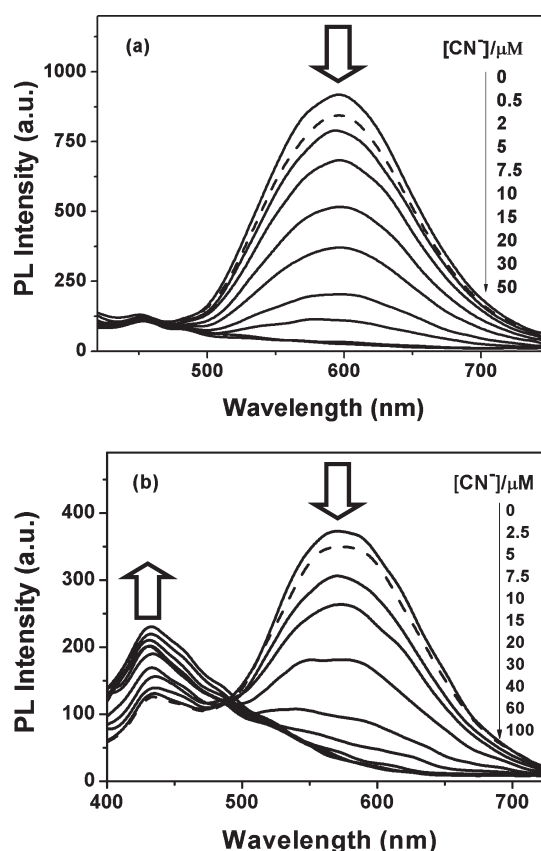


Figure 4. Fluorescence spectral changes of **P1** (a) and **M1** (b) with the increasing concentrations of CN^- in DMF. Excitation wavelength of **P1** and **M1** was 400 and 380 nm, respectively.

and polymer **P1** changed remarkably (Figure 1b). **M1** showed a major emission peak at 575 nm and only a very weak emission peak at 434 nm. The PL peaks of **P1** were further red-shifted to 597 and 455 nm, respectively. These new largely red-shifted PL peaks of **M1** and **P1** may be due to strong intramolecular charge transfer (ICT) interaction caused by the introduction of the very strong electron-withdrawing dicyano-vinyl group. As a result, bright yellow fluorescence and orange fluorescence was observed clearly for **M1** and **P1**, respectively. Furthermore, introduction of the strong electron-withdrawing group also resulted in the decreased fluorescence quantum yield. Fluorescence quantum yields of **M1** and **P1** were only 0.3% and 0.4%, respectively, which were much lower than those of their precursors (11% for **M0** and 13% for **P0**).

Sensing Properties. To exploit their sensing behaviors, their absorption spectral changes upon addition of various anions were investigated at first. 20 equiv of anions was added to the dilute DMF solutions ($5\ \mu\text{M}$) of **P1** and incubated for 10 min at room temperature. Dramatic change of the absorption spectrum induced by CN^- was observed, while almost no changes could be found in presence of other anions, including Cl^- , Br^- , I^- , H_2PO_4^- , HSO_4^- , and OAc^- , except for the very slight disturbances of F^- ions (Figure 2a). Upon adding CN^- , the intensity of the absorption peak of **P1** at 403 nm gradually decreased following the formation of a new band centered at 338 nm, and an isosbestic point at 360 nm was observed (Figure S1 in Supporting Information), which implied a new species with less conjugation was formed as we expected. More importantly, the

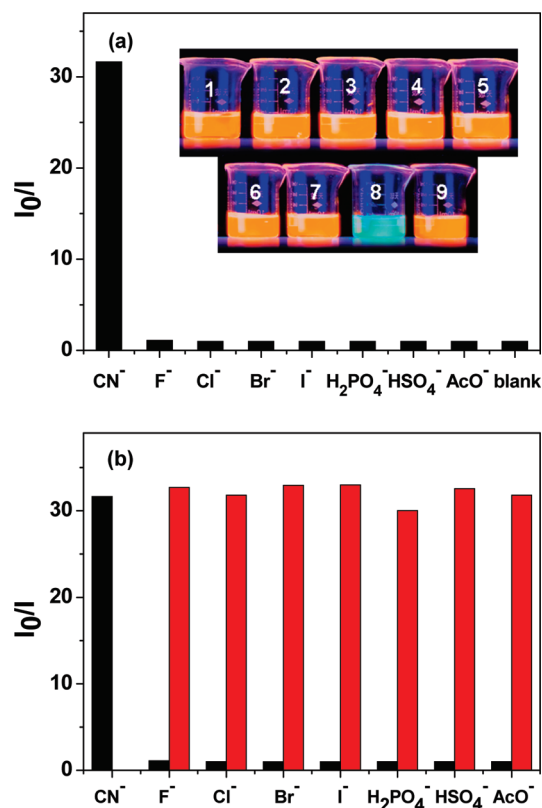


Figure 5. (a) Fluorescence response profiles of **P1** ($5\ \mu\text{M}$) at 597 nm in the presence of 20 equiv of each anions as Bu_4N^+ salts within 10 min. Inset: emission images observed for **P1** solutions upon addition of each anion: 1, F^- ; 2, Cl^- ; 3, Br^- ; 4, I^- ; 5, HSO_4^- ; 6, H_2PO_4^- ; 7, AcO^- ; 8, CN^- ; 9, **P1** only. (b) Response profiles of the **P1** with 20 equiv of each anions (black bar), followed by 20 equiv of CN^- (red bar).

color change from yellow-green to colorless can be clearly observed by the naked eye, while the other anions did not induce any significant color change, which suggests that naked-eye selective detection of CN^- becomes possible. (Figure 2b). The similar spectral behaviors occurred in **M1** solution of the same concentrations (Figure 3). However, the color changes of the **M1** ($5\ \mu\text{M}$) solution were not as obvious as that of **P1** solution due to its pale yellow color. At the same time, no change could be observed for absorption spectra of both **M0** and **P0** solutions upon the addition of all these anions, indicating the importance of the dicyano-vinyl group.

The CN^- sensing property was further examined through fluorescent titration studies in detail. Upon addition of CN^- to the **P1** solution, the PL intensity at 597 nm was quenched gradually, while the PL peak at 455 nm kept stable, suggesting the new species will only quenching the longer wavelength emission, which is also consistent with our design (Figure 4a). Finally, a 31.6-fold PL quenching was reached as its limit value after adding $50\ \mu\text{M}$ CN^- . In the range of $0.5\text{--}30\ \mu\text{M}$ cyanide concentration, the plot of the logarithm of the PL intensity at 597 nm as a function of the cyanide concentration showed a good linear relationship ($R^2 = 0.99$, Figure S2 in Supporting Information). This indicated that **P1** could be used to quantitatively detect CN^- concentration. Moreover, **P1** showed high sensitivity toward CN^- , and the detection limit was as low as $0.5\ \mu\text{M}$ (14 ppb), which was among the best results for CN^- sensing by fluorescence CP-based sensors reported so far. Similar fluorescence

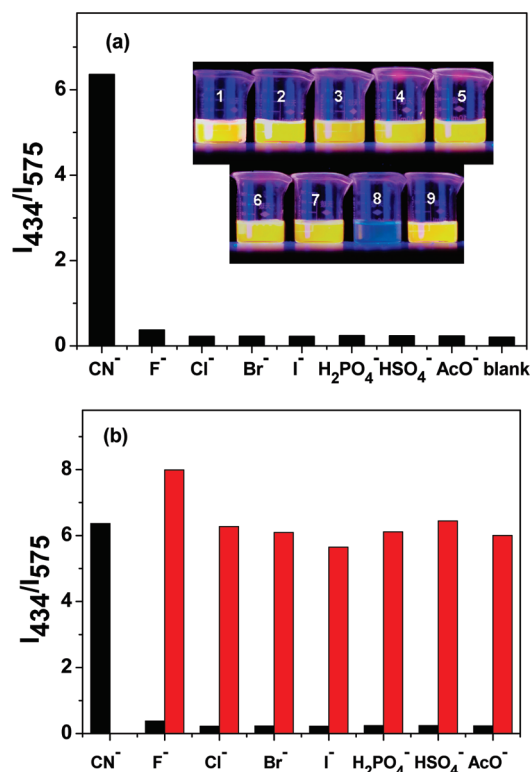


Figure 6. (a) Ratio fluorescence responses (I_{434}/I_{575}) of **M1** ($5\ \mu\text{M}$) in the presence of 20 equiv of each anion in DMF. Inset: emission images observed for **M1** solutions upon addition of each anion: 1, F^- ; 2, Cl^- ; 3, Br^- ; 4, I^- ; 5, HSO_4^- ; 6, H_2PO_4^- ; 7, AcO^- ; 8, CN^- ; 9, **M1** only. (b) Ratio fluorescence responses (I_{434}/I_{575}) of **M1** in the presence of different anions ($100\ \mu\text{M}$) (black bar), followed by addition of cyanide anion ($100\ \mu\text{M}$) (red bar).

titrations were also carried out in **M1** solution. Unlike **P1**, **M1** showed a ratiometric fluorescence response (Figure 4b). After adding CN^- , the PL intensity of the 575 nm emission decreased, while the PL intensity of the 434 nm emission increased. A 10.3-fold PL quenching at 575 nm and a 1.8-fold PL enhancement at 434 nm were observed when the cyanide concentration reached $100\ \mu\text{M}$. Considering the 31.6-fold PL quenching of **P1**, it is obvious that **P1** has higher sensitivity than **M1**, as most CP-based sensors. The emission intensity ratio, I_{434}/I_{575} , increased with the increase of cyanide concentrations, which allowed the detection of CN^- ratiometrically (Figure S3 in Supporting Information). Its detection limit was $2.5\ \mu\text{M}$ (70 ppb), which was much larger than that of **P1** (14 ppb), also indicating the higher sensitivity of **P1**. Additionally, the linear region of **M1** ($2.5\text{--}20\ \mu\text{M}$) was also narrower than that of **P1** ($0.5\text{--}30\ \mu\text{M}$).

The selectivity of the fluorescent response of **P1** ($5\ \mu\text{M}$) was verified in the presence of $100\ \mu\text{M}$ different anions, such as CN^- , F^- , Cl^- , Br^- , I^- , H_2PO_4^- , HSO_4^- , and OAc^- . As shown in Figure 5a, the PL of **P1** was practically insensitive to all of the anions, except for CN^- . In all these cases, the orange emission of **P1** was retained without any change, while the emission color suddenly changed to blue upon addition of CN^- . The excellent selectivity of **P1** was further highlighted by competition experiments. The PL intensity in the presence of CN^- was hardly changed by the coexistence of $100\ \mu\text{M}$ completing anions (Figure 5b). Under the same conditions, **M1** also displayed the good selectivity toward CN^- (Figure 6a). However, a more than

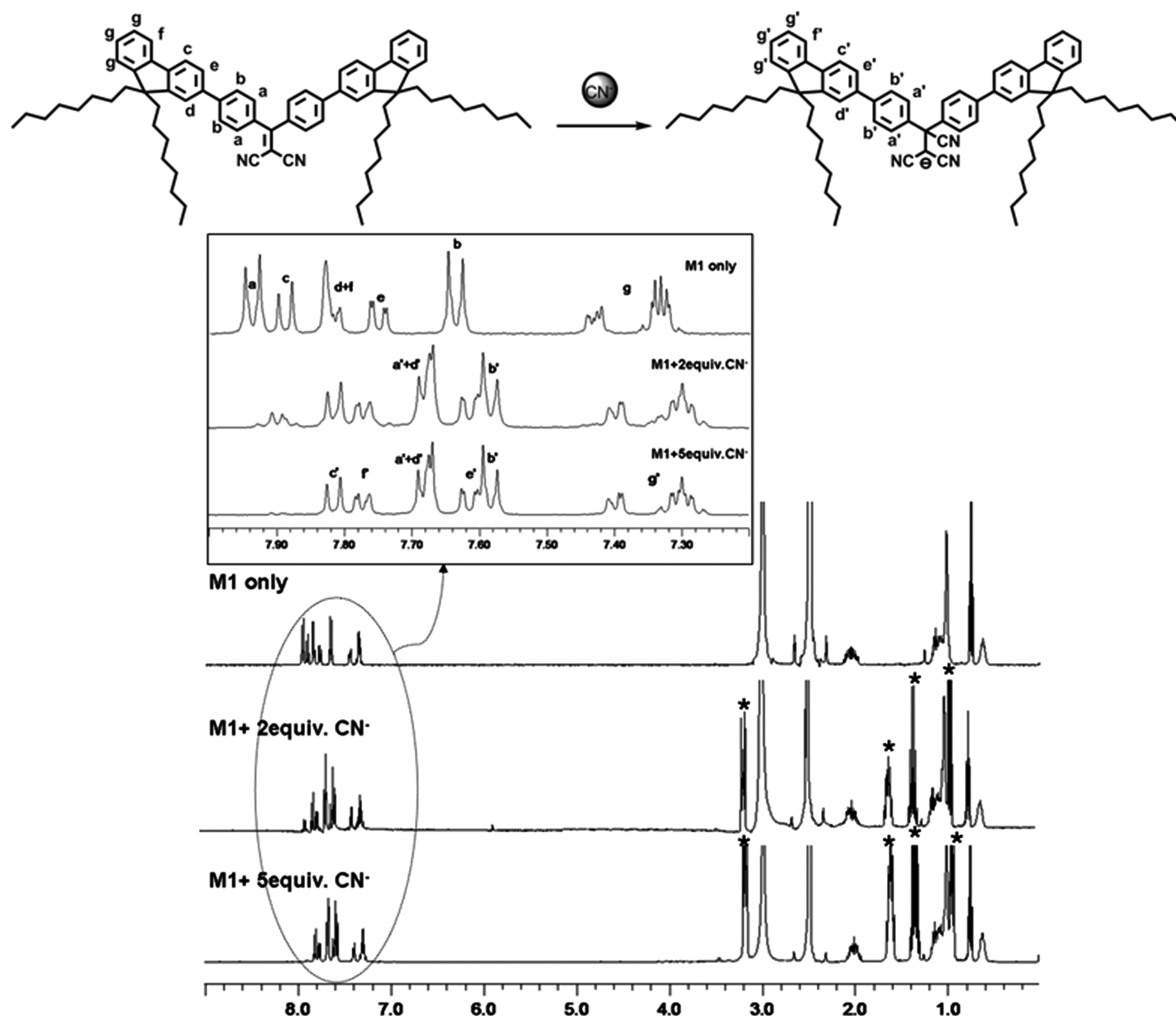


Figure 7. ^1H NMR spectral changes upon the addition of cyanide anion to **M1** (1.0 mM) in $\text{DMSO}-d_6$. (The peaks marked by asterisks (*) are attributed to the butyl group of Bu_4N^+ salts.) Inset: the expanded view of ^1H NMR spectral changes in the low fields. (The letters marked to the peaks in the figure correspond to the letters tagged on the schematic drawing of the proposed sensing mechanism.)

10% perturbation by F^- on the PL response is observed for **M1** in the competition experiment, indicating that **P1** even had a better selectivity for CN^- (Figure 6b). Anyway, it is obvious that the high selectivity of the chemodosimetric sensor is preserved in this CP-based sensor. Furthermore, the addition of various nucleophilic reagents (100 μM), such as diisopropylamine, *n*-propylamine, benzenethiol, sodium phenolate, and sodium azide, etc., lead to no absorption and fluorescence change for both **M1** and **P1**, indicating their extremely high selectivity to CN^- again.

To gain further insight into the nature of **P1**–cyanide interactions, we monitored the changes of ^1H NMR spectra and MALDI-TOF mass spectra produced via the addition of cyanide anion to **M1** solution. Addition of CN^- to a $\text{DMSO}-d_6$ solution (1 mM) of **M1** resulted in upfield shift of aromatic proton signal due to the breaking of the conjugation (Figure 7). A MALDI-TOF mass spectrometry of negative ions mode revealed two major components, which were identified as **M1** (calculated for $[\text{M1}]^-$, 1006.7; found, 1006.8) and its cyanide adduct

(calculated for $[\text{M1} + \text{CN}]^-$, 1032.7; found, 1032.7). All these observations clearly indicated that the cyanide anion was added to the vinyl group, and the anionic species was formed. In addition, the Job plot of **M1** and CN^- also supported a 1:1 binding stoichiometry (Figure S4 in Supporting Information).

The time-dependent fluorescence changes of **P1** and **M1** upon addition of 100 μM cyanide at room temperature were monitored to study their response rates to CN^- (Figures S7 and S8 in Supporting Information). The PL intensities of both **P1** and **M1** changed quickly and remained constant after 10 min, demonstrating their high reactivity. Although it is difficult to compare their rate constants (a polymer and a compound) for cyanide addition, we really noticed that the PL intensity of the major emission peak decreased by 50% in 65 s for **P1** and 106 s for **M1**, respectively (Figure 8), which implies that **P1** responded to CN^- more rapidly than **M1**. However, the PL response of **P1** to CN^- in $\text{DMF}-\text{H}_2\text{O}$ ($v/v = 95:5$) solution was rather slowly (Figure S10 in Supporting Information): its PL intensity was

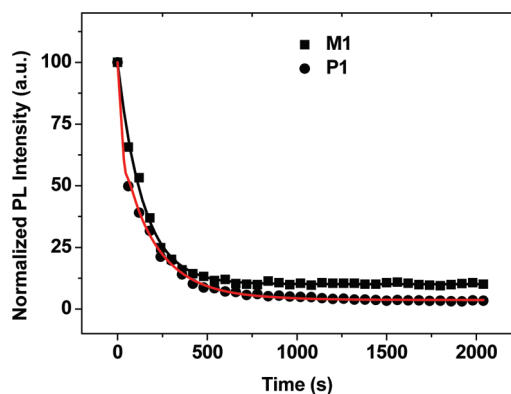


Figure 8. Time-dependent fluorescence intensity changes at 575 nm for **M1** and at 597 nm for **P1** upon addition of 20 equiv of cyanide anion to **M1** and **P1** in DMF. The time when the PL intensity of the major emission peak decreased to half ($I_{1/2}$) was calculated according to the fitting curves. $I_{1/2} = I_0 - (I_0 - I_{\infty})/2$. I_0 was the fluorescence intensity in the absence of added CN^- , and I_{∞} was the stable value of fluorescence intensity after addition of CN^- .

only quenched by 25% in 2 h after adding CN^- , perhaps because the strong hydration of anion will weaken the nucleophilicity of CN^- .^{6g,8i} At the same condition, all the other anions simply did not have any effect on the absorption and PL spectra of **P1**, indicating that the high selectivity is preserved in the DMF- H_2O (v/v = 95:5) solution.

CONCLUSION

In summary, we have designed and synthesized a novel fluorescent CP-based chemodosimetric sensor **P1** for cyanide. Based on the nucleophilic addition reaction between the dicyanovinyl group and cyanide, **P1** showed high selectivity for cyanide over other common anions and could recognize cyanide by naked eye and fluorescence. Compared to its model compound **M1**, the amplified fluorescence response of **P1** was successfully demonstrated, and its detection limit for CN^- could be down to 14 ppb, which was among the best results for CN^- sensing by fluorescence CP-based sensors to the best of our knowledge. The better sensing performance of **P1** over **M1** was further confirmed by its lower detection limit, wider linear region, better competitive selectivity, and more rapid PL response. Most importantly, the combination of CP-based sensors and chemodosimetric sensors may provide a possible way to develop highly sensitive and selective fluorescence probes for cyanide anion and other analytes.

ASSOCIATED CONTENT

S Supporting Information. Additional UV-vis absorption, fluorescence data of **P1** and **M1**. This material is available free of charge via the Internet at <http://pubs.acs.org>.

ACKNOWLEDGMENT

This work is supported by the National Natural Science Foundation of China (Nos. 20904055, 21074130, and 50633040), the Science Fund for Creative Research Groups (No. 20921061), and the 973 Project (No. 2009CB623601).

REFERENCES

- (1) (a) McQuade, D. T.; Pullen, A. E.; Swager, T. M. *Chem. Rev.* **2000**, *100*, 2537–2574. (b) Thomas, S. W., III; Joly, G. D.; Swager, T. M. *Chem. Rev.* **2007**, *107*, 1339–1386. (c) Fan, L. J.; Zhang, Y.; Murphy, C. B.; Angell, S. E.; Parker, M. F. L.; Flynn, B. R.; Jones, W. E. *Coord. Chem. Rev.* **2009**, *253*, 410–422. (d) Liu, Y.; Ogawa, K.; Schanze, K. S. *J. Photochem. Photobiol., C: Photochem. Rev.* **2009**, *10*, 173–190. (e) Lee, K.; Povlich, L. K.; Kim, J. *Analyst* **2010**, *135*, 2179–2189. (f) Li, K.; Liu, B. *Polym. Chem.* **2010**, *1*, 252–259. (g) Qin, C.; Wong, W.-Y.; Wang, L. *Macromolecules* **2011**, *44*, 483–489.
- (2) (a) Galbraith, E.; James, T. D. *Chem. Soc. Rev.* **2010**, *39*, 3831–3842. (b) Duke, R. M.; Veale, E. B.; Pfeffer, F. M.; Krugerc, P. E.; Gunnlaugsson, T. *Chem. Soc. Rev.* **2010**, *39*, 3936–3953. (c) Steed, J. W. *Chem. Soc. Rev.* **2009**, *38*, 506–519. (d) Gale, P. A. *Chem. Commun.* **2008**, 4525–4540. (e) Kim, S. K.; Kim, H. N.; Xiaoru, Z.; Lee, H. N.; Soh, J. H.; Swamyand, K. M. K.; Yoon, J. *Supramol. Chem.* **2007**, *19*, 221–227. (f) Lankshear, M. D.; Beer, P. D. *Coord. Chem. Rev.* **2006**, *250*, 3142–3160. (g) Yoon, J.; Kim, S. K.; Singh, N. J.; Kim, K. S. *Chem. Soc. Rev.* **2006**, *35*, 355–360. (h) O’Neil, E. J.; Smith, B. D. *Coord. Chem. Rev.* **2006**, *250*, 3068–3080. (i) Martínez-Máñez, R.; Sancenón, F. *Chem. Rev.* **2003**, *103*, 4419–4476.
- (3) (a) Harrison, B. S.; Ramey, M. B.; Reynolds, J. R.; Schanze, K. S. *J. Am. Chem. Soc.* **2000**, *122*, 8561–8562. (b) Ho, H. A.; Leclerc, M. *J. Am. Chem. Soc.* **2003**, *125*, 4412–4413. (c) Liu, Y.; Schanze, K. S. *Anal. Chem.* **2008**, *80*, 8605–8612. (d) Saxena, A.; Fujiki, M.; Rai, R.; Kim, S.-Y.; Kwak, G. *Macromol. Rapid Commun.* **2004**, *25*, 1771–1775. (e) Naito, M.; Nakamura, M.; Terao, K.; Kawabe, T.; Fujiki, M. *Macromolecules* **2010**, *43*, 7919–7923. (f) Bonifácio, V. D. B.; Morgado, J.; Scherf, U. *J. Polym. Sci., Part A: Polym. Chem.* **2008**, *46*, 2878–2883. (g) Tong, H.; Wang, L.; Jing, X.; Wang, F. *Macromolecules* **2003**, *36*, 2584–2586. (h) Zhou, G.; Cheng, Y.; Wang, L.; Jing, X.; Wang, F. *Macromolecules* **2005**, *38*, 2148–2153. (i) Vetrichelvan, M.; Nagarajan, R.; Valiyaveetil, S. *Macromolecules* **2006**, *39*, 8303–8310.
- (4) (a) Kim, I. B.; Han, M. H.; Phillips, R. L.; Samanta, B.; Rotello, V. M.; Zhang, Z. J.; Bunz, U. H. F. *Chem.—Eur. J.* **2009**, *15*, 449–456. (b) Wu, C.-Y.; Chen, M.-S.; Lin, C.-A.; Lin, S.-C.; Sun, S.-S. *Chem.—Eur. J.* **2006**, *12*, 2263–2269. (c) Chu, Q.; Medvetz, D. A.; Pang, Y. *Chem. Mater.* **2007**, *19*, 6421–6429. (d) Zhu, L.; Yang, C.; Zhang, W.; Qin, J. *Polymer* **2008**, *49*, 217–224. (e) Qu, Y.; Hua, J.; Jiang, Y.; Tian, H. *J. Polym. Sci., Part A: Polym. Chem.* **2009**, *47*, 1544–1552. (f) Sakai, R.; Okade, S.; Barasa, E. B.; Kakuchi, R.; Ziabka, M.; Umeda, S.; Tsuda, K.; Satoh, T.; Kakuchi, T. *Macromolecules* **2010**, *43*, 7406–6429.
- (5) (a) Zeng, Q.; Cai, P.; Li, Z.; Qin, J.; Tang, B. Z. *Chem. Commun.* **2008**, 1094–1096. (b) Li, Z.; Lou, X.; Yu, H.; Li, Z.; Qin, J. *Macromolecules* **2008**, *41*, 7433–7439. (c) Yang, R.; Wu, W.; Wang, W.; Li, Z.; Qin, J. *Macromol. Chem. Phys.* **2010**, *211*, 18–26. (d) Tian, Y. Q.; Chen, C. I. Y.; Yang, C. C.; Young, A. C.; Jang, S. H.; Chen, W. C.; Jen, A. K. Y. *Chem. Mater.* **2008**, *20*, 1977–1987. (e) Zhao, X.; Liu, Y.; Schanze, K. S. *Chem. Commun.* **2007**, 2914–2916.
- (6) (a) Xu, Z.; Chen, X.; Kim, H. N.; Yoon, J. *Chem. Soc. Rev.* **2010**, *39*, 127–137. (b) Badugu, R.; Lakowicz, J. R.; Geddes, C. D. *J. Am. Chem. Soc.* **2005**, *127*, 3635–3641. (c) Qian, G.; Li, X. Z.; Wang, Z. Y. *J. Mater. Chem.* **2009**, *19*, 522–530. (d) Männel-Croisé, C.; Probst, B.; Zelder, F. *Anal. Chem.* **2009**, *81*, 9493–9498. (e) Peng, L. H.; Wang, M.; Zhang, G. X.; Zhang, D. Q.; Zhu, D. B. *Org. Lett.* **2009**, *11*, 1943–1946. (f) Vallejos, S.; Estevez, P.; Garcia, F. C.; Serna, F.; de la Pena, J. L.; Garcia, J. M. *Chem. Commun.* **2010**, 46, 7951–7953. (g) Kim, D.-S.; Chung, Y.-M.; Jun, M.; Ahn, K. H. *J. Org. Chem.* **2009**, *74*, 4849–4854.
- (7) *Guidelines for Drinking-Water Quality*, 3rd ed.; World Health Organization: Geneva, 2004.
- (8) (a) Ros-Lis, J. V.; Martínez-Máñez, R.; Soto, J. *Chem. Commun.* **2002**, 2248–2249. (b) Chung, Y. M.; Raman, B.; Kim, D.-S.; Ahn, K. H. *Chem. Commun.* **2006**, 186–188. (c) Yang, Y.-K.; Tae, J. *Org. Lett.* **2006**, *8*, 5721–5723. (d) Lee, K.-S.; Kim, H.-J.; Kim, G.-H.; Shin, I.; Hong, J.-I. *Org. Lett.* **2008**, *10*, 49–51. (e) Cho, D.-G.; Kim, J. H.; Sessler, J. L. *J. Am. Chem. Soc.* **2008**, *130*, 12163–12167. (f) Kim, S.-H.; Hong, S.-J.; Yoo, J.; Kim, S. K.; Sessler, J. L.; Lee, C.-H. *Org. Lett.* **2009**, *11*, 3626–3629. (g) Jo, J.; Lee, D. *J. Am. Chem. Soc.* **2009**, *131*, 16283–16291. (h) Park, S.;

- Kim, H.-J. *Chem. Commun.* **2010**, 46, 9197–9199. (i) Lou, B.; Chen, Z.-Q.; Bian, Z.-Q.; Huang, C.-H. *New J. Chem.* **2010**, 34, 132–136. (j) Chung, Y. M.; Raman, B.; Kim, D.-S.; Ahn, K. H. *Chem. Commun.* **2006**, 186–188.
- (9) Kim, T.-H.; Swager, T. M. *Angew. Chem., Int. Ed.* **2003**, 42, 4803–4806.
- (10) Hong, S.-J.; Yoo, J.; Kim, S.-H.; Kim, J. S.; Yoong, J.; Lee, C.-H. *Chem. Commun.* **2009**, 189–191.
- (11) Li, S.; Zhao, P.; Huang, Y.; Li, T.; Tang, C.; Zhu, R.; Zhao, L.; Fan, Q.; Huang, S.; Xu, Z.; Huang, W. *J. Polym. Sci., Part A: Polym. Chem.* **2009**, 47, 2500–2508.
- (12) Xin, Y.; Wen, G.; Zeng, W.; Zhao, L.; Zhu, X.; Fan, Q.; Feng, J.; Wang, L.; Wei, W.; Peng, B.; Cao, Y.; Huang, W. *Macromolecules* **2005**, 38, 6755–6758.